Hysteresis and synchronization processes of Kuramoto oscillators on high-dimensional simplicial complexes with competing simplex-encoded couplings

Malayaja Chutani,[1] Bosiljka Tadić,[2,3] and Neelima Gupte[1,4]
[1]*Department of Physics, Indian Institute of Technology Madras, Chennai 600036, India*
[2]*Department of Theoretical Physics, Jožef Stefan Institute, Ljubljana, Slovenia*
[3]*Complexity Science Hub Vienna, Vienna, Austria*
[4]*Complex Systems and Dynamics Group, Indian Institute of Technology Madras, Chennai 600036, India*

(Received 19 May 2021; accepted 24 August 2021; published 7 September 2021)

Recent studies of dynamic properties in complex systems point out the profound impact of hidden geometry features known as simplicial complexes, which enable geometrically conditioned many-body interactions. Studies of collective behaviors on the controlled-structure complexes can reveal the subtle interplay of geometry and dynamics. Here we investigate the phase synchronization (Kuramoto) dynamics under the competing interactions embedded on 1-simplex (edges) and 2-simplex (triangles) faces of a homogeneous four-dimensional simplicial complex. Its underlying network is a 1-hyperbolic graph with the assortative correlations among the node's degrees and the spectral dimension that exceeds $d_s = 4$. By numerically solving the set of coupled equations for the phase oscillators associated with the network nodes, we determine the time-averaged system's order parameter to characterize the synchronization level. Our results reveal a variety of synchronization and desynchronization scenarios, including partially synchronized states and nonsymmetrical hysteresis loops, depending on the sign and strength of the pairwise interactions and the geometric frustrations promoted by couplings on triangle faces. For substantial triangle-based interactions, the frustration effects prevail, preventing the complete synchronization and the abrupt desynchronization transition disappears. These findings shed new light on the mechanisms by which the high-dimensional simplicial complexes in natural systems, such as human connectomes, can modulate their native synchronization processes.

DOI: 10.1103/PhysRevE.104.034206

I. INTRODUCTION

In complex systems, collective dynamics is a marked signature of emerging properties related to complex structure, studied by mapping onto networks [1]. The synchronization of oscillator systems is a paradigmatic stochastic process for study the emergence of coherent behavior in many natural and laboratory systems [2]. In recent years, research focuses on the system's hidden geometry features [3,4] and their impact on dynamics. Notably, new dynamical phenomena appear that can be related to the higher-order connectivity and interactions supported by the system's hidden geometry, which is mathematically described by simplicial complexes [5–11].

A formal theory of the simplicial complexes of graphs [12–14] defines a simplicial complex as a structure consisting of different simplexes, e.g., n-cliques, which share one or more common nodes representing a geometrical face of the implicated simplexes. For example, an n-clique is a full graph of n nodes, and its faces are simplexes of the order $q = 0, 1, 2, 3, ...q_{\max}$, where $q_{\max} = n$-1 defines the dimension of the simplex. Hence, the dimension of the simplicial complex is defined by the order of the largest simplex that it contains. Recent studies revealed simplicial architecture in networks mapping many complex systems from the brain [15–18], designed materials [19], and physics problems [20–23] to structures emerging from online social endeavors [24] and large-scale social networks [25,26]. Such simplicial structure naturally underlies many-body interactions [6] and, more generally, nonlinear couplings that cannot be reduced to pairwise interactions [27]. However, revealing the mechanisms by which such high-dimensional simplicial complexes determine collective dynamics in these complex systems represents a challenging problem. For example, patterns of brain circuits that perform complex integration or segregation processes are known to involve larger distributed structures of brain areas, hypersimplexes [28], as well as smaller densely connected groups recognized as cliques and cavities [29,30]. Such cliques appear to form hierarchically organized simplicial complexes in the human connectome [16,17]. At the same time, powerful imaging techniques revealed that the brain functions, in particular the cognition processes, are closely related with the appearance of brain rhythms and a large-scale neural synchronization, represented by multichannel phase correlations (see Ref. [31] and references therein). In the opinion paper [31], the authors stated that "the study of brain rhythms and synchronisation of oscillatory activity is currently one of the hottest topics in neuroscience," calling for computational modeling and nonlinear dynamics analysis.

In this context, the generative models of high-dimensional simplicial complexes of a controlled structure are of great importance [32–35]. For example, in the model of self-assembly of cliques of different size developed in Ref. [32], the assembly is controlled by two factors. These are the geometric compatibility of the attaching clique's faces with the once already built into the growing structure and the chemical affinity toward the addition of new nodes. Varying the chemical affinity, one can grow different structures from sparsely connected cliques that share a single node to the very dense structure of large cliques sharing their most prominent subclique, see the online demo in Ref. [34]. Moreover, the architecture of simplicial complexes manifests on several unique properties of the underlying network (1-skeleton of the simplicial complex), which can affect the pairwise interaction, see Sec. II for details. For example, the network's spectral dimension can vary from the values close to the tree graphs in sparsely connected cliques of any size to the values $d_s \geqslant 4$ in the case of large densely connected cliques, as shown in Ref. [36]. Hence, the structure-dynamics interplay can be expected both because of the pairwise and higher-order interactions due to the actual architecture of simplicial complexes. More precisely, it has been demonstrated by studies of spin kinetics [7,8], contagious dynamics [11], and synchronization processes [9,10,37] on various simplicial complexes. Notably, in the field-driven magnetization reversal on simplicial complexes [7,8], the antiferromagnetic interactions via links of the triangle faces provide strong geometric frustration effects that determine the shape of the hysteresis loop. The higher-order interactions then affect its symmetry; meanwhile, the width of the hysteresis remains strictly determined by the dimension of the simplicial complex. In the contagious and synchronization processes, on the other hand, the appearance of the hysteresis loop is strictly related to the higher-order interactions. The synchronization has been studied extensively on a variety of networks [2,38] using an ensemble of phase oscillators (Kuramoto model) with interactions via network edges. It has been understood that the onset of synchronous behavior can be affected by the local connectivity and correlations among the nodes [39], and global features captured by the network's spectral dimension [40]. The nature of synchronization transition can depend on the process' sensitivity to the sign of interactions, time delay, and the frustration effects causing new phenomena [41–46]. Furthermore, the presence of higher-order interactions are shown to induce an abrupt desynchronization, depending on the dimension of the dynamical variable and the range of couplings [9,10]. It remains unexplored how the coincidental interactions of a different order, encoded by the faces of a large simplicial complex, cooperate during the synchronization processes.

Here we tackle this problem by numerical investigations of synchronization and desynchronization processes among Kuramoto phase oscillators considering the leading interactions based on 1-simplices (edges) and 2-simplices (triangles) as the faces of homogeneous four-dimensional simplicial complexes. The structure is grown by self-assembly of 5-cliques that preferably share the most extensive face. The underlying graph of this simplicial complex possesses several unique features. These are hyperbolicity, assortative mixing, and a high spectral dimension, allowing complete synchronization when the positive pairwise interaction is increased. Our results suggest that these geometrical properties, even in the absence of the higher-order interactions, can lead to new states with partial synchronization, mainly when the pairwise coupling is negative, which can be attributed to frustration. Furthermore, these simplex-based interactions have competing effects, leading to different patterns of synchronization and desynchronization. Remarkably, the triangle-based interactions tend to hinder the synchronization processes promoted by the increasing pairwise coupling, leading to the hysteresis loop and the abrupt desynchronization when the fully synchronized state can be reached, i.e., for a moderate strength of interaction. Both the complete synchrony and the abrupt desynchronization disappear for strong triangle-based interactions, suggesting the dominance of geometric frustration.

In Sec. II, we present the relevant details of the structure of the simplicial complex and the underlying network. Section III introduces the dynamical model with the simplex-based interactions and discusses the case with pairwise interaction alone. In Sec. IV, the effects of the triangle-based interactions on the order-parameter and hysteresis loop are shown. Section V presents a summary and discussion of the results.

II. NETWORK GEOMETRY UNDERLYING SYNCHRONIZATION PROCESSES

As mentioned in the Introduction, we use the algorithm of cooperative self-assembly introduced in Refs. [32,34] to grow a simplicial complex (SC) by an assembly of 5-cliques, i.e., full graphs of the size $n = 5 = q_{\max} + 1$. The network growth starts with a single clique; then, each new clique is attached by sharing its q-face with one of the existing cliques. The remaining $q_{\max} - q$ nodes are added to form that clique on the growing network (cf. online demo [34]). The geometric compatibility of its faces determines the attachment rules of a new clique to the growing structure with the currently built-in cliques; besides, the chemical affinity parameter ν modulates the probability of binding along a q-dimensional face. Specifically, the probability that the clique of the order $q_{\max}$ attaches by sharing its q-face is given by [32] $P(q_{\max}, q; t) = \frac{c_q(t)e^{-\nu(q_{\max}-q)}}{\sum_{q=0}^{q_{\max}-1} c_q(t)e^{-\nu(q_{\max}-q)}}$, where $C_q(t)$ is the number of geometrically compatible locations of the order q at the step t. For $\nu = 0$, the leading probability is determined by strictly geometric factor $C_q(t)$, whereas, for negative values of the chemical affinity $\nu < 0$, the maximum probability corresponds to the largest number of added nodes $q_{\max} - q$; thus, the cliques preferably share a single-node face. Oppositely, the increasing positive affinity parameter favors sharing larger faces, as the larger probability corresponds to decreasing number of added nodes $q_{\max} - q$. Here we used a large positive value $\nu = +5$. Thus, the newly added clique mainly consists of a new node and a 4-clique face shared with the previously added clique. An example of the resulting compact structure consisting of 5-cliques is shown in Fig. 1 (top left). To assess the relevance of a particular network property in the observed collective dynamics, we also study the synchronization of phase oscillators on two randomized versions of our simplicial complex. Specifically, we perform random rewiring that preserves the

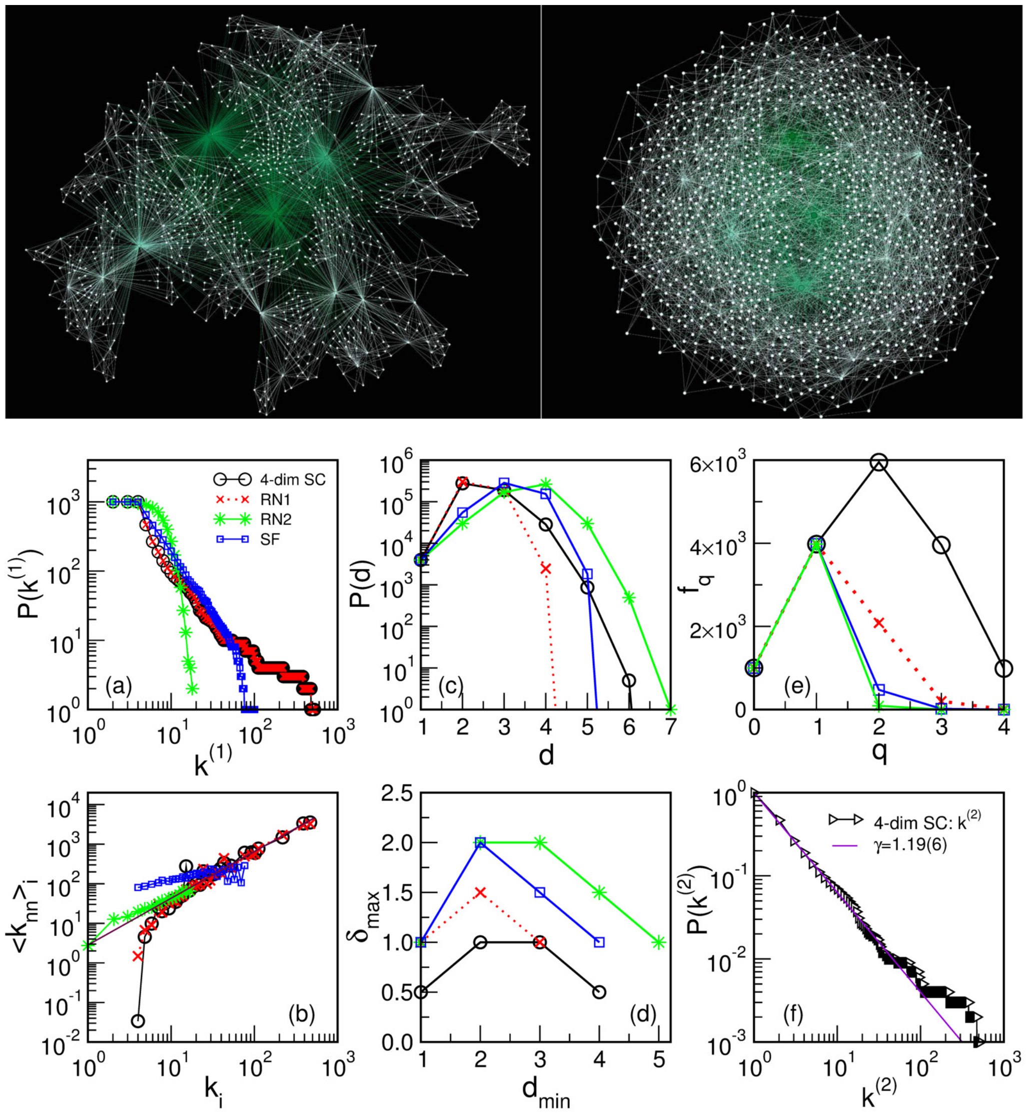

FIG. 1. Visualization of the homogeneous four-dimensional simplicial complex SC of 1000 nodes (top left) and the structure randomized to preserve the nodes degree, RN1 (top right). Panels (a)–(e) show different structural properties, in particular the cumulative distribution of the node's degree (a), assortativity (b), the distribution of the shortest path distances (c), the maximum hyperbolicity parameter (d), and the number of faces of different orders $q = 0, 1, 2 \cdots 4$ up to the maximal cliques (e). Different symbols (colors) are for the original four-dimensional SC, and the networks of the same size with the degree-preserving randomized structure RN1, the fully randomized structure RN2, and the simple scale-free network with the matching slope, SF. The same legend applies to panels (a)–(e). Panel (f) shows the normalized distribution of the number of triangles per node (generalized degree) in the four-dimensional SC.

degree of each node (the network is also shown in Fig. 1 (top right) and a fully randomized structure. For further comparison, we also consider a simple scale-free network with the power-law exponent that coincides with the slope observed in the degree distribution of the SC for the intermediate degree, cf. Fig. 1.

Besides the high spectral dimension of our SC, $d_s \geqslant 4$ shown in Ref. [36], several other structural measures of these networks relevant to the synchronization dynamics are given in Figs. 1(a)–1(f). Figure 1(e) shows that even though they all contain the same number of nodes ($q = 0$) and a similar number of edges ($q = 1$ simplexes), they significantly differ in the presence of higher simplexes. Specifically, a small number of triangles ($q = 2$ simplexes) as the highest structures appear in the entirely random graph. Similarly, the simple scale-free network possesses a small number of triangles and no higher structures. On the other hand, the degree-preserving randomized network still possesses about 30% of the triangles compared to the original simplicial complex and a few tetrahedrons ($q = 3$ simplexes). Meanwhile, the number of tetrahedrons and 5-cliques in the original complex is comparable to the number of edges and nodes, respectively. The distribution of the number of triangles in which a given node participates, also known as generalized degree $k_i^{(2)}$, of our simplicial complex is shown in the panel Fig. 1(f). Besides the four hubs with many triangles attached to them, the remaining part of the distribution obeys an algebraic decay with the increasing $k_i^{(2)}$.

At the level of edges, the underlying graph of our simplicial complex exhibits some characteristic features depicted in Figs. 1(a)–1(d) in comparison with the other three structures. Specifically, it exhibits a wide range of the degree $k_i \equiv k_i^{(1)}$ with a few large-degree nodes. In the intermediate range, the cumulative degree distribution has a power-law decay with the exponent $\gamma \sim 1.81 \pm 0.05$, matched by the generated scale-free network, see Fig. 1(a). Naturally, the degree-preserved randomized structure obeys the same degree distribution; meanwhile, the exponentially decaying distribution characterises the fully randomized structure. Moreover, our network possesses the assortative mixing among the neighboring node's degree [47]; it is quantified by the positive exponent $\mu > 0$ in the expression $\langle k_{nn} \rangle_i \sim k_i^{\mu}$ for the average degree of the neighbours of a node i as a function of the node's i degree, suggesting that the nodes of similar connectivity are mutually connected. Figure 1(b) shows the assortative feature with $\mu \sim 1.19 \pm 0.06$ for the graph of our simplicial complex. Notably, statistically similar assortative correlations are present in the degree-preserving randomized structure. Meanwhile, the random graph and the simple scale-free networks have $\mu \sim 0$ compatible with the absence of degree correlations. Furthermore, Figs. 1(c) and 1(d) shows that, in the graph's metric space (endowed with the shortest-path distance), these graphs have a relatively small diameter and hyperbolicity or negative curvature [48,49]; more precisely, they are δ-hyperbolic with a small δ value [50,51]. Moreover, due to the attachments among cliques [52], which are 0-hyperbolic objects, it was shown [32] that the topological graphs of the emergent assembly are always 1-hyperbolic. Practically, this means that the maximum observed δ in the Gromov hyperbolicity criterion [50] cannot exceed the value 1 for any four-tuple of nodes in that graph. In Fig. 1(d) we show how the $\delta_{\max}$ can vary with the minimal distance in a large number of sampled four-tuples for all four network structures. Notably, $\delta_{\max} = 1$ for the graph of our simplicial complex, as expected, and it increases by 1/2 with the degree-preserving randomization of edges. In the small-δ graphs, such increases of the hyperbolicity parameter are attributed [51] to the appearance of a characteristic subjacent structure, usually a new cycle compatible with the new δ value. Our graph's complete randomization and the simple scale-free structure appear to possess even larger cycles, resulting in the $\delta_{\max} = 2$. In the following two sections, we will investigate the synchronization processes among phase oscillators interacting via edges and triangles of these networks.

III. PHASE SYNCHRONIZATION WITH THE COMPETING SIMPLEX-BASED INTERACTIONS

The phase variable is an angle defined on a unit circle, θ_i, associated with the network's nodes $i = 1, 2, 3, \ldots, N$. The local interactions among these dynamical variables of the strengths K_q are provided by the network's topology elements, which are strictly related to the corresponding faces of the simplicial complex. In this work, we consider two leading interactions associated with the edges ($q = 1$) and interactions among triplets located on a triangle face ($q = 2$), with the strength K_1 and K_2, respectively. The evolution equations given by

$$\dot{\theta}_i = \omega_i + \frac{K_1}{k_i^{(1)}} \sum_{j=1}^{N} A_{ij} \sin(\theta_j - \theta_i) + \frac{K_2}{2k_i^{(2)}} \sum_{j=1}^{N} \sum_{l=1}^{N} B_{ijl} \sin(\theta_j + \theta_l - 2\theta_i) \tag{1}$$

are coupled via the two interaction terms. In particular, A_{ij} is an element of the 1-simplex adjacency matrix $\mathbf{A}$, such that $A_{ij} = 1$ if nodes i, j are conneted by a link and 0 otherwise; meanwhile, B_{ijl} is an element of the 2-simplex adjacency tensor $\mathbf{B}$, such that $B_{ijl} = 1$ if nodes i, j, l belong to a common 2-simplex and 0 otherwise. The normalization factors in Eq. (1) are the respective simplex degree of a node, $k_i^{(q)}$, i.e., number of distinct q-simplices that node i is part of. Specifically, $k_i^{(1)}$ is the number of 1-simplices (edges) incident on node i, and $k_i^{(2)}$ is the number of 2-simplices (triangles) incident on node i. Thus, equal weightage is given to all the terms contributing to the sum in each interaction term. It is important to note the number of edges and the number of triangles per node in the underlying graph of our simplicial complex obey a broad (partly a power-law) distribution, cf. Figs. 1(a) and 1(f). In Eq. (1), ω_i is the intrinsic frequency of the ith oscillator, which dictates its motion when there is no interaction with other oscillators in the network. The pairwise interactions seek to reduce the difference between the phase of the ith oscillator and each of its neighboring oscillators when $K_1 > 0$. In contrast, the oscillators tend toward opposite phases when $K_1 < 0$. The third term, representing three-node interactions of the ith oscillator based on each 2-simplex incident on node i, is a natural generalization of the pairwise interaction term [10]. It should be stressed that the interactions between these three nodes occur over faces of the simplicial complex and not over any given three nodes. Furthermore, this interaction term is symmetric in i, in that it is unaffected by permutations in the other two indices. Revealing the impact of the 2-simplex term in Eq. (1) on the synchronization processes that are promoted by the pairwise interactions is one of the objectives of this work.

As it is widely accepted, the degree of synchronization of the whole network is quantified by the Kuramoto order parameter

$$r = \left\langle \left| \frac{1}{N} \sum_{j=1}^{N} e^{i\theta_j} \right| \right\rangle, \tag{2}$$

where the brackets $\langle \cdot \rangle$ indicate the time average. Hence, $r = 1$ represents the perfect synchronization, i.e., all phases are equal, and $r = 0$ in the disordered phase. Meanwhile, the stable states with $0 < r < 1$ indicate the presence of more complex patterns and partial synchronization.

In the simulations, for each network node $i = 1, 2, \ldots, N$, where we have $N = 1000$, the initial conditions are set for θ_i and ω_i as the uniform random number in the range $\theta_i \in [0, 2\pi]$ and the Gaussian random number with a zero mean and unit variance, respectively. The numerical solution of the set of equations (1) is performed using a numerical integrating function `odeint` from Python's SciPy library [53]. This

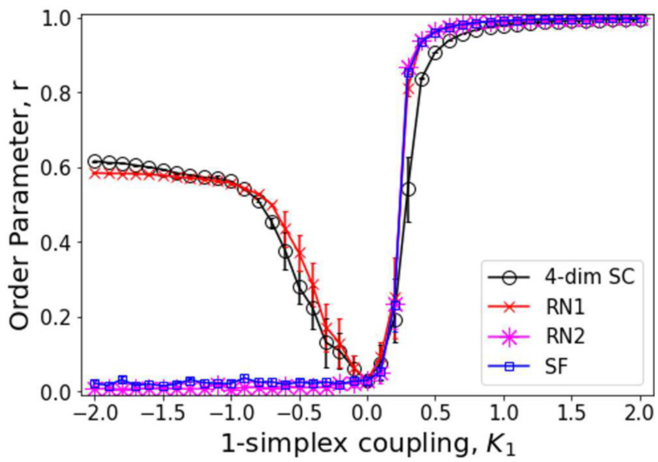

FIG. 2. The order parameter r as a function of the 1-simplex coupling strength K_1 without the higher-order interactions. Different lines and symbols are for four-dimensional simplicial complex (○), randomized network with the original degree distribution (×), fully randomized network (⋆), and a simple scale-free network with the same number of nodes and edges (□).

function integrates a system of ordinary differential equations (ODEs) using the `lsoda` solver from the Fortran library ODEPACK. It solves ODEs with the Adams (predictor-corrector) method the backward differentiation formula for nonstiff and stiff cases, respectively. For each set of parameter values, the system is iterated for 50 000 steps, with the time step $d_t = 0.01$. The last 20 000 iterations are used to calculate the order parameter as in Eq. (2). Further, to study hysteresis, we track the system's trajectory as the coupling parameter K_1 is first adiabatically increased and then decreased. The step size of the coupling K_1 is taken to be 0.1. Alternatively, K_2 is varied in a suitable range, meanwhile fixing several representative K_1 values, as described in the second part of Sec. IV. A detailed program flow is given in the Appendix.

A. The case $K_2 = 0$: Synchronization under exclusively pairwise interactions

Before considering the competing simplex-based interactions, we will describe the synchronization process under the pairwise interactions alone, i.e., when $K_2 = 0$ in Eq. (1). As mentioned, these interactions are enabled by the edges of the substrate network, which is the 1-skeleton of our four-dimensional simplicial complex. Hence, different network features from local to global level are expected to play a role in the cooperative behaviors, depending on the interaction strength K_1. For the four-dimensional simplicial complex, as K_1 is increased from zero up to $K_1 = 2.0$, and we observe a continuous transition from a desynchronized state ($r \approx 0$) to a completely synchronized state ($r \approx 1$), see Fig. 2. On the other hand, with the negative values of K_1 decreased from $K_1 = 0$ to $K_1 = -2.0$, the order-parameter increases in a different manner and reaches the value $r \approx 0.6$, comprising a partially synchronized state. To demonstrate what network property can be responsible for the observed synchronization properties, we performed the simulations on the two randomized versions of the network, as described in Sec. II. Notably, for the degree-preserving randomized structure, RN1, qualitatively similar behavior of the order parameter is found. In contrast, for the fully randomized network, the order parameter remains zero for all values of $K_1 \leqslant 0$. Interestingly, almost identical values of the order-parameter compatible with the absence of synchronization at negative pairwise interactions are found in a simple scale-free network, as shown in Fig. 2. Therefore, we can conclude that the node's assortative degree correlations in the network of our simplicial complex and in the corresponding degree-preserving randomized version, cf. Fig. 1(b), can be responsible for the appearance of the partial synchronization for the negative pairwise interaction.

The distribution of phases over nodes, or the synchronization pattern, is expected to depend on the structure. Here, the histograms of phases corresponding to different representative values of the coupling strength K_1 are shown in Fig. 3 for different network structures. For a fair comparison of different cases (the same network with different coupling strength and different networks with the same coupling strength), the phases are taken after 50 000 time steps, always starting from the same initial conditions (the same sequence of random numbers). While the order parameter in the scale-free and entirely random network is practically identical, cf. Fig. 2, the histograms of phases in the synchronized state shown in Fig. 3 appear to be different; this is in accordance with different evolution times to reach complete synchrony, which can be attributed to the degree distribution as the only measurable difference between these networks. On the other hand, there is a remarkable similarity in the distribution of phases in the simplicial-complex network and its degree-preserving randomized version. Moreover, the peak for large positive values of K_1 is close to the one seen in the corresponding scale-free structure with the same power-law exponent. These findings suggest the relevance of the network's degree distribution to the outcome distribution of phases when the complete synchrony can occur in the absence of higher-order couplings. Investigating the pattern of phases in the network and the precise role of individual nodes in its development exceeds this work's scope. On the negative K_1 side, the majority of phases also appear to be in the same region; see the top two rows of Fig. 3. How the partially synchronized state in these correlated networks appears is another vital issue. We anticipate that a large number of triangles, as shown in Fig. 1(e), can be responsible for the frustration effects leading to the partially synchronized states in these two networks. In the following, we will examine the impact of the triangle-based interactions in our simplicial complex.

IV. HYSTERESIS LOOP INDUCED BY HIGHER-ORDER INTERACTIONS

In this section, we will focus attention on synchronization dynamics on our network in the presence of triangle-based interactions, i.e., using $K_2 \neq 0$ in Eq. (1). We plot the time averaged order parameter r as a function of 1-simplex coupling K_1, for different 2-simplex coupling values $K_2 = 0.0, 0.2, 0.4, 0.5, 0.8, 1.0$ in Fig. 4. In these plots, first K_1 is increased adiabatically from $K_1 = -2.0$ to $+2.0$ (forward sweep), and then decreased from $K_1 = +2.0$ to -2.0

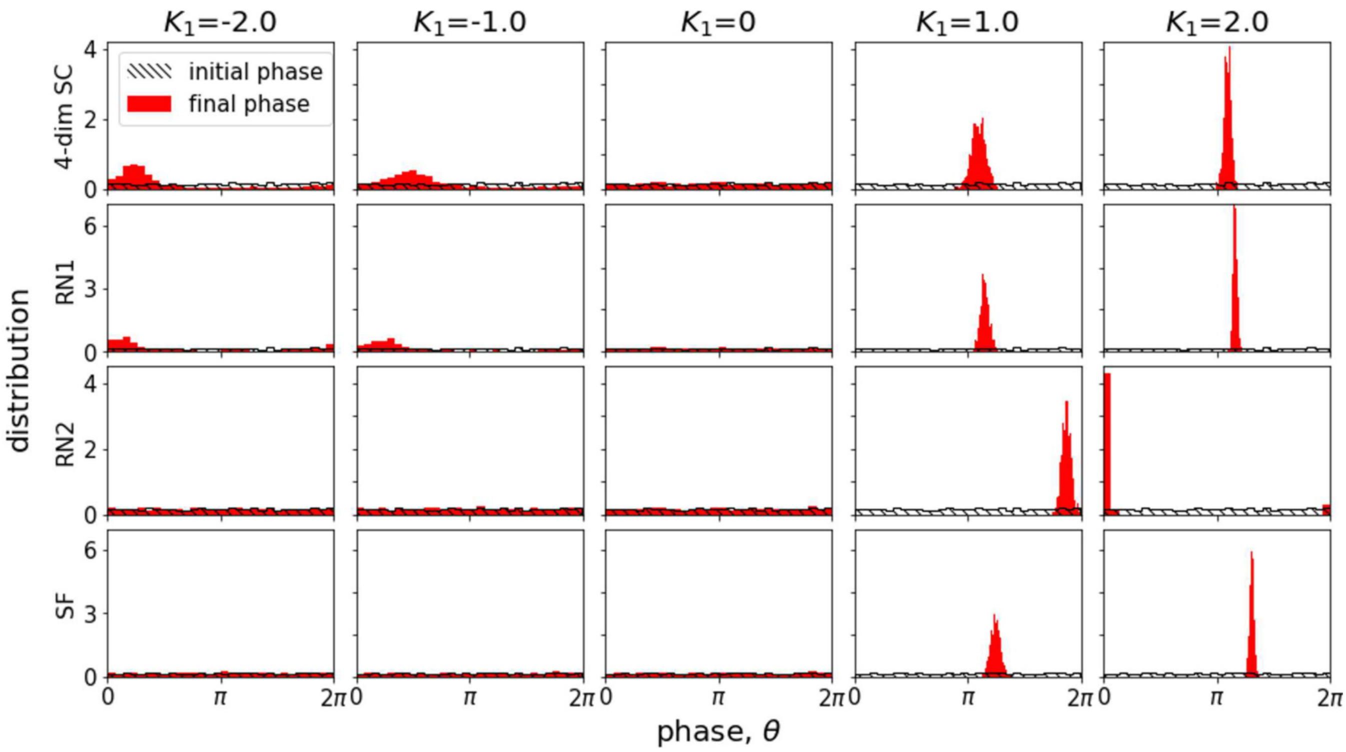

FIG. 3. Distribution of phases (measured in radians) in the initial (black, shading) and final (red, solid pattern) states of the synchronization simulations for different values of the pairwise interaction for four network structures described in Sec. II, always starting with the same initial conditions. The first row of panels is for the network of the four-dimensional simplicial complex, the second row is for the randomized network with the original degree distribution (RN1), the third row is for the fully randomized network (RN2), and the last row is for the scale-free network (SF), all of which have the same number of nodes and edges.

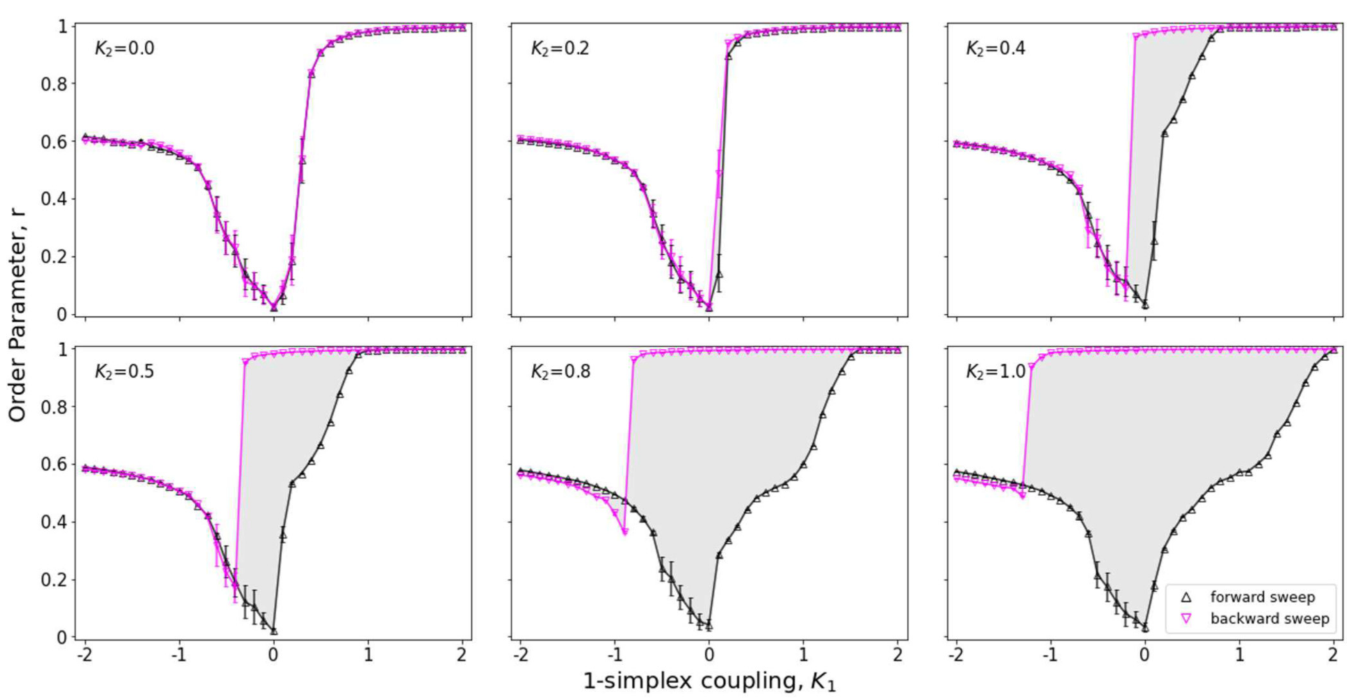

FIG. 4. Synchronization with higher-order interactions: Hysteresis sweep of the order parameter as a function of 1-simplex coupling strength K_1 for different 2-simplex coupling strength K_2 values. As the value of K_2 increases, we notice an increase in the size of the hysteresis loop.

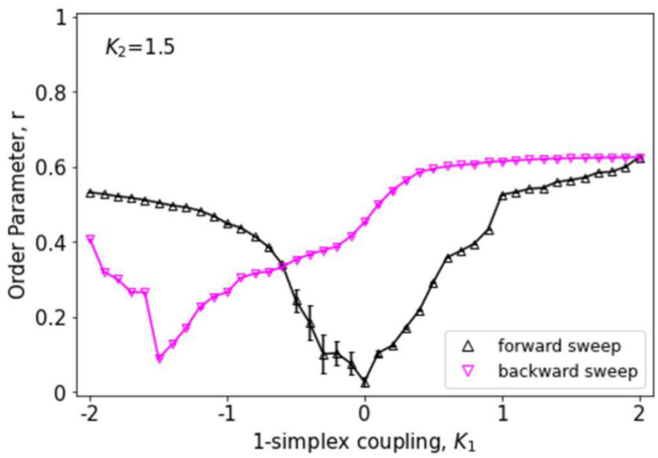

FIG. 5. Hysteresis loop for strong 2-simplex interaction K_2: Only partial synchronization is accessible even at a large positive K_1; the abrupt desynchronization disappears.

(backward sweep) in steps of $dK_1 = 0.1$. For each plot shown in Fig. 4, we see that at $K_1 = -2$, the system is partially synchronized, with a finite r value. The system gradually desynchronizes as K_1 tends toward zero. Next, as K_1 is increased toward $+2.0$, a continuous increase of the level of synchronization occurs. For higher values of K_2, the transition remains continuous but the growth of the order parameter slows down in the region around $K_1 \sim 0.5$ and gradually reaches the complete synchrony at larger values of K_1. In the backward sweep, as K_1 decreases from $+2.0$ to zero and further toward $K_1 = -2$, the desynchronization transition largely depends on the value of the triangle-based interactions. Namely, when $K_2 = 0$, the transition is continuous following the same trajectory as the forward transition, through the fully desynchronized state at $K_1 = 0$, and ending up with the partially synchronized state at $K_1 = -2$. As the coupling K_2 is increased, the forward and backward transitions are no longer reversible. More precisely, when $K_2 \gtrsim 0.4$, the 2-simplex interactions come into effect by slowing down the level of synchronization in the forward sweep, as mentioned above. The underlying dynamical mechanisms remain to be investigated; some preliminary results suggest the emergence of different clusters in this range of competing interactions. Meanwhile, in the backward sweep, we note a discontinuous desynchronization decay toward the $K_1 < 0$ branch. The occurrence of an abrupt desynchronization has been previously reported in Refs. [5,9,10] as a prominent effect of higher-order interactions with different coupling types. In this context, the abrupt destruction of the synchronized state in our simplicial complex is also expected. What is new is the specific dependence of the hysteresis loop and thus the abrupt desynchronization phenomenon on the strength of the 2-simplex interactions, as demonstrated by the results in Figs. 4 and 5. The abrupt transition is to a partially synchronized state with a nonzero value of the order parameter. Notably, an abrupt decay of the completely synchronized state occurs when K_2 is large enough to balance the effects of the nonpositive pairwise interaction $K_1 \leqslant 0$. Thus, the only complete desynchronization transition appears at the point $K_1 = 0$ for a small K_2 value, as Fig. 4 shows. Figure 4 shows that, beyond this value of K_2, the hysteresis loop grows in size as K_2 is increased, affecting both the forward sweep at the positive K_1 side and the size of the first-order jump. This scenario continues for a wider range of values of the 2-simplex interaction strength as long as the large positive pairwise interactions are sufficient to maintain a complete synchrony. However, for larger values of K_2, the fully synchronized state is no longer accessible; instead, a kind of partial synchronization is reached under the competing interactions. The backward sweep from such a state, as shown in Fig. 5, closes up an entirely different shape of the hysteresis loop with two distinct parts at positive and negative K_1, and continuous changes of the order parameter. Hence, we can conclude that the impact of the 2-simplex encoded interactions on our four-dimensional simplicial complex strongly depends on the sign and strength of the pairwise interactions. An overview of its effects is displayed in Fig. 6, and discussed in Sec. V.

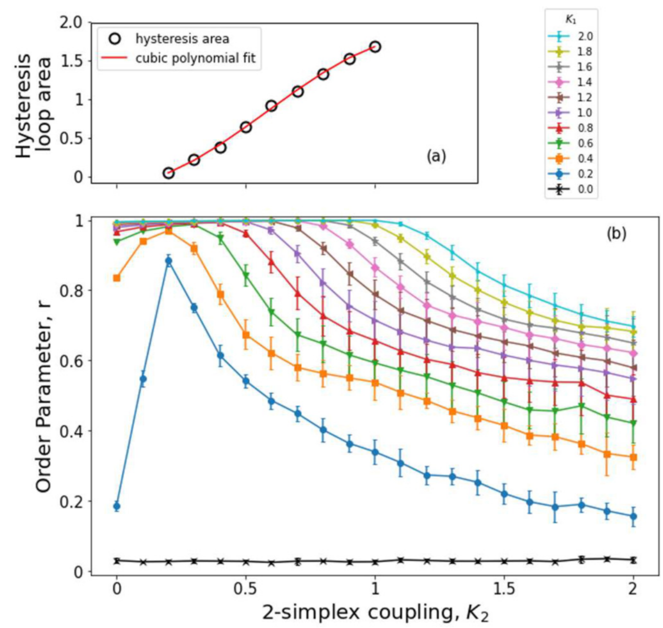

FIG. 6. (a) The size of the hysteresis loop obtained by increasing and then decreasing pairwise interaction K_1, as shown in Fig. 4, plotted against K_2; the parameters of the cubic polynomial fit are given in the text. (b) The order parameter r against K_2 for increasing (bottom to top lines) values of K_1 indicated in the legend.

Furthermore, we analyze how the hysteresis loop area grows with increasing K_2. Particularly, we plot the area of the hysteresis loops for different values of K_2 against K_2 in Fig. 6(a). The curve is best fitted with a cubic function $f(x) = -2.3767K_2^3 + 4.1631K_2^2 - 0.0050K_2 - 0.1043$ with root-mean-square error 0.01866.

We highlight the competing nature of the 1-simplex and 2-simplex interactions. To that end, we carry out synchronization simulations for different pairs of coupling strengths K_1 and K_2, illustrated by plotting the order parameter, r, as a function of 2-simplex coupling K_2 in Fig. 6(b). We notice that the order parameter remains negligible if the pairwise interactions are absent, $K_1 = 0$, for all values of K_2 considered, suggesting that the 2-simplex interactions alone cannot induce the system's synchronization. Next, we notice that for finite but low values of K_1, increasing K_2 leads to higher synchronization but only until around $K_2 \leqslant 0.2$. A further increase in K_2 leads to decreasing the system's level of synchronization, as seen from the decaying values of r with K_2. Note that higher K_1 are gradually needed to compete with the desynchronizing effects due to high K_2. Subsequently, the curves of r in Fig. 6(b) decrease with the increasing K_2. In this range of K_2 values, the complete synchrony is no longer accessible, as also demonstrated with the hysteresis loop in Fig. 5.

V. DISCUSSION AND CONCLUSIONS

How high-dimensional simplicial complexes can shape the dynamics is a question of great relevance to many functional systems. Among these, a prominent example is the human connectome structure underlying the brain functional complexity [16,17,29,30]. To address this issue, we have studied the processes of phase synchronization on a homogeneous four-dimensional simplicial complex of a given size (10^3 nodes); we have considered the leading interactions encoded by 1-simplex (edges) and 2-simplex (triangles) faces and varying the respective strengths K_1 and K_2. Our results revealed a variety of scenarios for the synchronization and desynchronization (both to complete and partially desynchronized states), depending on the sign of the pairwise interactions and the geometric frustration promoted by the triangle-based interactions. The latter can be attributed to the actual organization of 5-cliques that make the simplicial complex; notably, every link in this complex is a shared face of at least three triangles. In addition, the 1-skeleton of this simplicial complex that enables pairwise interactions has specific geometrical properties. Apart from the high spectral dimension [36], the assortative degree correlations play their role in the synchronization processes, as discussed above in Sec. III A. Moreover, the graph's hyperbolicity is a salient feature of these simplicial complexes [32,52], cf. Sec. II.

More precisely, we have demonstrated that:

(i) the 1-simplex interactions of both signs $K_1 \gtrless 0$ promote the synchronization but with different mechanisms; no synchrony can arise due to 2-simplex interactions alone;

(ii) for $K_1 > 0$ the two interaction types have competing effects, and the complete synchrony can be reached for a moderate range of K_2, balanced by the increasingly stronger pairwise coupling K_1;

(iii) for the negative pairwise interactions $K_1 < 0$, however, the 2-simplex interactions support the mechanisms leading to partially ordered states due to K_1;

(iv) the prominent impact of the 2-simplex interactions is seen in the opening-up of the hysteresis loop and the appearance of a finite jump in the backward sweep starting from the completely synchronized state, in analogy to the abrupt desynchronization found in other studies [5,9,35]. Note that, in our case, the desynchronization is partial following the forward branch for $K_1 \leqslant 0$, except when it occurs precisely at the point $K_1 = 0$;

(v) eventually, for substantial 2-simplex interactions $K_2 \gtrsim K^*$ the geometric frustration prevailed, leading to partial synchronization even though a large positive K_1 is applied; the abrupt desynchronization entirely disappears; on the negative $K_1 < 0$ side, a new segment of the hysteresis loop opens up, suggesting that potentially different orderings in the frustrated synchronization may be competing before a significant negative K_1 prevails. Finally, we note that the 2-simplex interactions do not promote additional order, cf. Fig. 6(b), and we expect that the loop closes up at the partial synchronization level determined by significant negative K_1; the final value $r \sim 0.52$ in Fig. 5 is determined numerically at $K_1 = -2$.

Our four-dimensional simplicial complex with the simplex-encoded interactions represent an excellent example to investigate how geometry influences the synchronization and desynchronization processes on it. Even though the studied higher-order interactions are the leading cause of new dynamical phenomena, the collective behavior's genesis is rooted in the pairwise interactions. Hence, certain nontrivial features of the underlying network are highly relevant. Our study sheds new light on the competing role of simplex-embedded interactions in high-dimensional simplicial complexes, which occur in many natural dynamical systems. As mentioned, the prominent example represents the brain dynamics, where current studies [16,17,28–31] clearly point out the connections between the network structure, captured by simplicial complexes, and the occurrence of a large-scale synchronization of the oscillatory activity related to brain functions. In this context, some outstanding questions remain for future study. For example, such questions regard the relative importance of the order of interactions that can be embedded in a given simplicial complex, and the type of hysteresis loop that may occur due to the competing higher-order interactions. Prompted by an anonymous reviewer, we point out a subject of particular interest to the community regarding the hysteresis loop due to the competing pairwise couplings of different signs and range of interactions embedded on the high-dimensional simplicial complexes. Moreover, our approach traces the ways to study the role of defect simplexes, the temporally varying simplicial architecture and distributed weights, which can have profound effects on collective dynamic behaviors.

ACKNOWLEDGMENTS

B.T. acknowledge financial support from the Slovenian Research Agency under the P1-0044 program. N.G. thanks IIT Madras for the CoE Project No. SP20210777DRMHRDDIRIIT. M.C. acknowledges the use of the computing resources at HPCE, IIT Madras.

APPENDIX

1. Program Flow

INPUT Graph $\mathscr{G}$, stored as an list of edges and list of triangles;
Initialize phases of the oscillators, θ_i, such that they are distributed uniformly between 0 and 2π;
Initialize intrinsic frequencies of the oscillators, ω_i, such that they are distributed normally, with zero mean and unit variance;
Set the value K_2. Assign $K_2 = 0$, if 2-simplex interactions are to be ignored. Assign finite K_2, if 2-simplex interactions are to be added;
Set the value $K_1 = -2.0$; Set the incremental change in K_1 to be $dK_1 = 0.1$;
`Forward sweep:`
while $K_1 \leqslant +2.0$ **do**
  for all nodes $i \in \mathscr{G}$ **do**
    solve the differential Eq. (1);
  end for
  Calculate order parameter for the system, using Eq. (2);
  Increase K_1 by dK_1;
end while
`Backward sweep:`
while $K_1 \geqslant -2.0$ **do**
  for all nodes $i \in \mathscr{G}$ **do**
    solve the differential Eq. (1);
  end for
  Calculate order parameter for the system, using Eq. (2);
  Decrease K_1 by dK_1;
end while
END

[1] R. M. D'Souza, J. Gomez-Gardenes, J. Nagler, and A. Arenas, Explosive phenomena in complex networks, Adv. Phys. **68**, 123 (2019).

[2] F. A. Rodrigues, T. K. DM. Peron, P. Ji, and J. Kurths, The kuramoto model in complex networks, Phys. Rep. **610**, 1 (2016).

[3] M. Boguna *et al.*, Network geometry, Nat. Rev. Phys. **3**, 114 (2021).

[4] D. C. da Silva, G. Bianconi, R. A. da Costa, S. N. Dorogovtsev, and J. F. F. Mendes, Complex network view of evolving manifolds, Phys. Rev. E **97**, 032316 (2018).

[5] P. S. Skardal and A. Arenas, Higher order interactions in complex networks of phase oscillators promote abrupt synchronization switching, Commun. Phys. **3**, 218 (2020).

[6] F. Battiston *et al.*, Networks beyond pairwise interactions: Structure and dynamics, Phys. Rep. **874**, 1 (2020).

[7] B. Tadić, M. Andjelković, M. Šuvakov, and G. J. Rodgers, Magnetisation processes in geometrically frustrated spin networks with self-assembled cliques, Entropy **22**, 336 (2020).

[8] B. Tadić and N. Gupte, Hidden geometry and dynamics of complex networks: Spin reversal in nanoassemblies with pairwise and triangle-based interactions, Europhys. Lett. **132**, 60008 (2020).

[9] P. S. Skardal and A. Arenas, Abrupt Desynchronization and Extensive Multistability in Globally Coupled Oscillator Simplexes, Phys. Rev. Lett. **122**, 248301 (2019).

[10] X. Dai, K. Kovalenko, M. Molodyk, Z. Wang, X. Li, D. Musatov *et al.*, D-dimensional oscillators in simplicial structures: Odd and even dimensions display different synchronization scenarios Chaos, Solitons Fractals **146**, 110888 (2021).

[11] A. Arenas, W. Cota, J. Gómez-Gardeñes, S. Gómez, C. Granell, J. T. Matamalas, D. Soriano-Panos, and B. Steinegger, Modeling the Spatiotemporal Epidemic Spreading of Covid-19 and the Impact of Mobility and Social Distancing Interventions, Phys. Rev. X **10**, 041055 (2020).

[12] J. Jonsson, *Simplicial Complexes of Graphs*, Lecture Notes in Mathematics (Springer-Verlag, Berlin, 2008).

[13] Y. Zhao and S. Maletić, *Simplicial Complexes in Complex Systems* (World Scientific, Singapore, 2021).

[14] J. R. Beaumont and A. C. Gatrell, *An Introduction to Q-analysis*, Concepts and Techniques in Modern Geography, no. 34. (Geo Abstracts, Norwich, 1982).

[15] B. Tadić, M. Andjelković, B. M. Boshkoska, and Z. Levnajić, Algebraic topology of multi-brain connectivity networks reveals dissimilarity in functional patterns during spoken communications, PLoS One **11**, e0166787 (2016).

[16] B. Tadić, M. Andjelković, and R. Melnik, Functional geometry of human connectomes, Sci. Rep. **9**, 12060 (2019).

[17] M. Andjelković, B. Tadić, and R. Melnik. The topology of higher-order complexes associated with brain hubs in human connectomes, Sci. Rep. **10**, 17320 (2020).

[18] Z. Moradimanesh, R. Khosrowabadi, M. Eshaghi Gordji, and G. R. Jafari, Altered structural balance of resting-state networks in autism, Sci. Rep. **11**, 1966 (2021).

[19] S. Ikeda and M. Kotani, Materials inspired by mathematics, Sci. Technol. Adv. Mater. **17**, 253 (2016).

[20] M. Andjelković, N. Gupte, and B. Tadić, Hidden geometry of traffic jamming, Phys. Rev. E **91**, 052817 (2015).

[21] B. Tadić, M. Andjelković, and M. Šuvakov, The influence of architecture of nanoparticle networks on collective charge transport revealed by the fractal time series and topology of phase space manifolds, J. Coupl. Syst. Multisc. Dynam. **4**, 30 (2016).

[22] G. Bianconi, C. Rahmede, and Z. Wu, Complex quantum network geometries: Evolution and phase transitions, Phys. Rev. E **92**, 022815 (2015).

[23] M. Chutani, N. Rao, N. Nirmal Thyagu, and N. Gupte, Characterizing the complexity of time series networks of dynamical systems: A simplicial approach, Chaos **30**, 013109 (2020).

[24] M. Andjelković, B. Tadić, M. Mitrović Dankulov, M. Rajković, and R. Melnik, Topology of innovation spaces in the knowledge networks emerging through questions-and-answers, PLoS One **11**, e0154655 (2016).

[25] U. Alvarez-Rodriguez *et al.*, Evolutionary Dynamics of Higher-order Interactions in Social Networks, Nature Human Behaviour **5**, 586 (2021).

[26] B. Tadić, Self-organised criticality and emergent hyperbolic networks: Blueprint for complexity in social dynamics, Eur. J. Phys. **40**, 024002 (2019).

[27] J. Petereit and A. Pikovsky, Chaos synchronization by nonlinear coupling, Commun. Nonlinear Sci. Numer. Simulat. **44**, 344 (2017).

[28] O. V. Maslennikov, D. S. Shchapin, and V. I. Nekorkin, Transient sequences in a hypernetwork generated by an adaptive network of spiking neurons, Philos. Trans. R. Soc. A **375**, 20160288 (2017).

[29] M. W. Reimann, M. Nolte, M. Scolamiero, K. Turner, R. Perin, G. Chindemi *et al.*, Cliques of neurons bound into cavities provide a missing link between structure and function, Front. Comput. Neurosci. **11**, 48 (2017).

[30] A. E. Sizemore, C. Giusti, A. Kahn, J. M. Vettel, R. F. Betzel, and D. S. Bassett. Cliques and cavities in human connectome, J. Comput. Neurosci. **44**, 115 (2018).

[31] R. Guevara Erra, J. L. Perez Velazquez, and M. Rosenblum, Neural synchronization from the persepective of non-linear dynamics, Front. Comput. Neurosci. **11**, 98 (2017).

[32] M. Šuvakov, M. Andjelković, and B. Tadić, Hidden geometries in networks arising from cooperative self-assembly, Sci. Rep. **8**, 1987 (2018).

[33] B. Tadić, M. Šuvakov, M. Andjelković, and G. J. Rodgers, Large-scale influence of defect bonds in geometrically constrained self-assembly, Phys. Rev. E **102**, 032307 (2020).

[34] M. Šuvakov, M. Andjelković, and B. Tadić, Applet: Simplex aggregated growing graph, 2017 (http://suki.ipb.rs/ggraph/).

[35] K. Kovalenko *et al.*, Growing scale-free simplices, Commun. Phys. **4**, 43 (2021).

[36] M. Mitrović Dankulov, B. Tadić, and R. Melnik, Spectral properties of hyperbolic networks with tunable aggregation of simplexes, Phys. Rev. E **100**, 012309 (2019).

[37] R. Ghorbanchian, J. Restrepo, J. J. Torres, and G. Bianconi, Higher-order simplicial synchronization of coupled topological signals, Commun. Phys. **4**, 120 (2021).

[38] A. Arenas, A. Díaz-Guilera, J. Kurths, Y. Moreno, and C. Zhou, Synchronization in complex networks, Phys. Rep. **469**, 93 (2008).

[39] P. Li, K. Zhang, X. Xu, J. Zhang, and M. Small, Reexamination of explosive synchronization in scale-free networks: The effect of disassortativity, Phys. Rev. E **87**, 042803 (2013).

[40] A. P. Millán, J. J. Torres, and G. Bianconi, Synchronization in network geometries with finite spectral dimension, Phys. Rev. E **99**, 022307 (2019).

[41] H. Wu and M. Dhamala, Dynamics of kuramoto oscillators with time-delayed positive and negative couplings, Phys. Rev. E **98**, 032221 (2018).

[42] F. Dai, S. Zhou, T. Peron, W. Lin, and P. Ji, Interplay among inertia, time delay, and frustration on synchronization dynamics, Phys. Rev. E **98**, 052218 (2018).

[43] S.-Y. Ha, D. Ko, and Y. Zhang, Emergence of phase-locking in the kuramoto model for identical oscillators with frustration, SIAM J. Appl. Dynam. Syst. **17**, 581 (2018).

[44] P. Khanra, P. Kundu, C. Hens, and P. Pal, Explosive synchronization in phase-frustrated multiplex networks, Phys. Rev. E **98**, 052315 (2018).

[45] D. Goldstein, M. Giver, and B. Chakraborty, Synchronization patterns in geometrically frustrated rings of relaxation oscillators, Chaos **25**, 123109 (2015).

[46] H. Xia, G. Jian, S. Yu-Ting, Z. Zhi-Gang, and X. Can, Effects of frustration on explosive synchronization, Front. Phys. **11**, 110504 (2016).

[47] S. Dorogovtsev, *Lectures on Complex Networks* (Oxford University Press, New York, 2010).

[48] O. Narayan and I. Saniee, Large-scale curvature of networks, Phys. Rev. E **84**, 066108 (2011).

[49] W. Chen, W. Fang, G. Hu, and M. W. Machoney, *On the Hyperbolicity of Small-world and Tree-like Random Graphs*, Lecture Notes in Computer Science, Vol. 7676 (Springer-Verlag, Berlin, 2012), pp. 278–288.

[50] S. Bermudo, J. M. Rodríguez, J. M. Sigarreta, and J.-M. Vilaire, Gromov hyperbolic graphs, Discr. Math. **313**, 1575 (2013).

[51] S. Bermudo, J. M. Rodríguez, O. Rosario, and J. M. Sigarreta, Small values of the hyperbolicity constant in graphs, Discr. Math. **339**, 3073 (2016).

[52] N. Cohen, D. Coudert, G. Ducoffe, and A. Lancin, Applying clique-decomposition for computing gromov hyperbolicity, Theor. Comput. Sci. **690**, 114 (2017).

[53] P. Virtanen, R. Gommers, T. E. Oliphant, M. Haberland, T. Reddy, D. Cournapeau *et al.*, *SciPy* 1.0: Fundamental algorithms for scientific computing in Python, Nat. Methods **17**, 261 (2020).